FORCE MEASUREMENT AND MODELING FOR MOTOR PROTEINS BETWEEN MICROSPHERE AND MICROFLUIDIC CHANNEL SURFACE

Ryuji Yokokawa[1,2*], Yusuke Sakai[1], Atsuhito Okonogi[1], Isaku Kanno[1] and Hidetoshi Kotera[1]
[1]Department of Microengineering, Kyoto University, Kyoto, JAPAN
[2]PRESTO JST, Kawaguchi, Saitama, JAPAN

ABSTRACT

This paper reports a fundamental study on a force measurement and mechanical modeling of a microbead coated with multiple motor proteins, kinesins, which moves on a cytoskeletal filament, microtubules (MTs). We utilized a laminar flow in a microfluidic channel to apply torque $\boldsymbol{\Gamma}$ and drag force $\boldsymbol{F_D}$ to the bead, whose values can be derived theoretically. As a result, the adhesion force $\boldsymbol{F_{Adh}}$ was determined based on the mechanical modeling. Here, the flow rate necessary to break kinesin-MT bindings was experimentally measured, and two models were applied to derive fluid forces that was also calculated by a simulation software, FLUENT. Consequently, adhesion forces of 363 pN and 31 pN were obtained under no ATP and 1 mM ATP conditions, respectively. The proposed measurement methodology is advantageous in analyzing multiple microbeads transported by kinesin-MT interaction in a microfluidic system.

KEYWORDS: Motor protein, force measurement, microfluidics, kinesin, microtubule (MT)

INTRODUCTION

Measurement of force acting between motor protein and cytoskeletal filament has been an attractive research target in biophysics field, which was typically measured by optical tweezers [1]. In practice, the optical trap capture a microbead coated by a single kinesin molecule, and bring the bead to a MT filament. Kinesin-MT interaction cause kinesin motility through ATP hydrolysis, in which the trap force and kinesin stall force are balanced. The balanced force can be determined by the bead displacement from the trap center and spring constant for the tweezers. This method provides high spacial and temporal resolution to reveal the motor behavior at the single molecule level. In contrast, active nanotransport of beads in a microfluidic system by the kinesin motility is achieved by multiple kinesins, because the cooperative work of multiple kinesins realizes longer and more stable transport than that done by one kinesin. In such a nanotransport system, it is necessary to evaluate multiple beads at a time to understand mechanics in the transport. Therefore, the optical tweezers method is not appropriate for simultaneous measurement, and statistical data is hardly obtained.

Here, we propose to utilize a stable laminar flow in a microfluidic channel. A drag force acting on an object in the flow can be estimated based on fundamental fluid dynamics. When a uniform flow velocity profile is given around a bead, Stokes drag force, $6\pi\mu aU$, is usually applied. Here, μ, a, and U are fluid viscosity, bead radius, and fluid velocity, respectively. However, this results in failure in our case due to the strong wall effect from the bottom glass surface. It is because the bead is attached on a glass surface with proteins in between, resulting in the small gap of several hundred nanometers. In order to take the effect into consideration for deriving drag force and torque, we calculated them based on two methods: when a bead was directly attached on the surface (analytical) [2], and lifted over the surface (partially numerical) [3]. They were also numerically calculated using 3-D laminar flow model with PC-based software, FLUENT 6.3, for comparison. For those calculations, flow rate to remove the beads from the glass surface was necessary to calculate forces. Therefore, in experimental section, ratio of microbeads attached and detached from the surface was measured corresponding to the calculated drag force. Applying a mechanical model proposed by S. Lorthois *et al*. [4] with some modification, we derived the adhesion force, $\boldsymbol{F_{Adh}}$. from torque $\boldsymbol{\Gamma}$ and drag force $\boldsymbol{F_D}$. We proposed to utilize a microfluidic system to realize parallel measurement of binding force between kinesin and MTs on multiple microbeads.

EXPERIMENTAL AND THEORETICAL FRAMEWORK

PDMS replica for a channel structure (w=500 μm, h=40 μm) was prepared by a standard molding technique using a SU-8 master mold. PDMS-coverglass bonding was realized by corona discharge. Tubulin and GST-tagged full-length kinesin were purified as described [5]. For fluorescence observations, rhodamine labeled tubulin was obtained. Purified tubulin was polymerized into MTs in BRB80 buffer (80 mM PIPES-NaOH pH=6.9, 1 mM $MgCl_2$, 1 mM EGTA) containing 1 mM $MgSO_4$ and 1 mM GTP incubating at 37ºC for 30 minutes. Stable flow (0-100 μL/min) was applied to the PDMS-coverslip microfluidic channel (Fig. 1), in which motor protein system with microbead was prepared [6]. The flow rate was increased gradually (1 μL/min), and the number of beads remaining on the glass surface was counted at each flow rate.

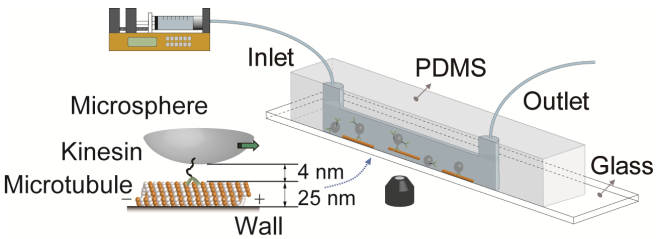

Figure 1: Experimental system. The PDMS-glass microchannel is fixed on an inverted microscope stage. Inlet is connected to a syringe pump to apply a pressure driven flow. Molecular system for the bead assay-based nanotransport.

The molecular binding is modeled as shown in Fig. 2 and Fig. 3. Drag force and torque were estimated by the following two methods. One is to neglect the protein size between the bead and surface (Fig. 3a), and the other is to consider the distance lifted for h from the wall due to proteins (Fig. 3b). Their drag force and torque are analytically derived using S for velocity gradient. Non-dimensional

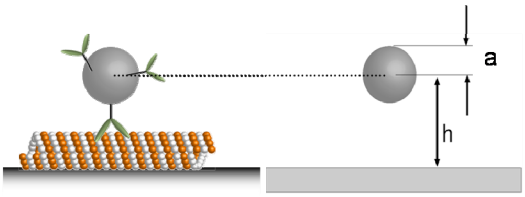

Figure 2: Schematic for the bead binding by kinesin-MT interaction. Bead radius, a, and distance from the glass surface to the bead center, h, are shown.

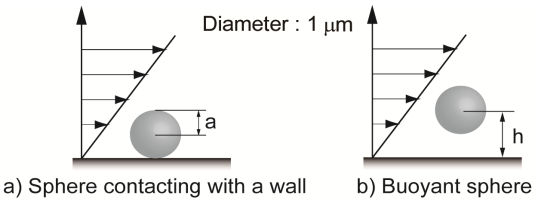

Figure 3: Two models to derive drag force and torque. Fig. 3a for $\boldsymbol{F_{D1}}$ and $\boldsymbol{\Gamma_1}$, Fig. 3b for $\boldsymbol{F_{D2}}$ and $\boldsymbol{\Gamma 2}$.

drag force, F_D^*, and torque, Γ^*, are functions of a non-dimensional parameter, *h/a*. Force and torque for two models are expressed as:

$$F_{D1} = 1.7009 \times 6\pi\mu a^2 S \quad (1)$$

$$\Gamma_1 = 0.943993 \times 4\pi\mu a^3 S \quad (2)$$

$$F_{D2} = 6\pi\mu ahSF_D^* \quad (3)$$

$$\Gamma_2 = 4\pi\mu a^3 S\Gamma^* \quad (4).$$

We evaluated these values by adopting an ideal molecular configuration: bead diameter ($2a$ = 1 μm), distance between bead and glass surface (45 nm), and resulting in h = 545 nm.

Since several kinesins are coated on the bead, kinesin-MT bindings are modeled as parallel springs as shown in Fig. 4. Shortest kinesin form is considered as 5% (4 nm) of fully extended kinesin, and longest one is 20% (16 nm) [6]. Force and momentum at the rotational axis were balanced, and $\boldsymbol{F_{Adh}}$ was derived (Fig. 4).

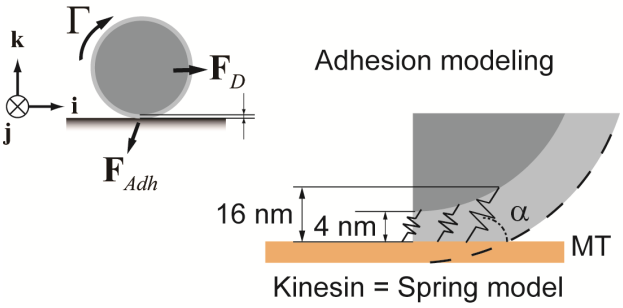

Figure 4: Experimental system. The PDMS-glass microchannel is fixed on an inverted microscope stage. Inlet is connected to a syringe pump, which controls the stable flow. Molecular system for the bead assay-based nanotransport.

$$F_{Adh} = |\boldsymbol{F_{Adh}}| = 2l_c wDE\lambda = \left(F_D^2 + \frac{(\Gamma + aF_D)^2}{l_c^2}\right)^{1/2} \quad (5)$$

Here, $\boldsymbol{F_D}$ and $\boldsymbol{\Gamma}$ for a given flow rate can be derived through the two models, and $\boldsymbol{l_c}$ depends on kinesin length bridging bead and MT. D: kinesin density, E: spring constant, w: MT diameter, and λ: extension of kinesin spring.

RESULTS and DISCUSSION

Figure 5 shows drag force calculated by two models and FLUENT. The flow rate range was optimized referring to the binding force in our experimental setup. Buoyant bead, $\boldsymbol{F_{D2}}$, (model Fig. 3b) showed a slight increase from a bead contacting with a wall, $\boldsymbol{F_{D1}}$, (model Fig. 3a) at the flow rate of 100 μl/min (Fig. 5), which is not negligible compared with a single kinesin force ~5.8 pN. Dependency of $\boldsymbol{F_D}$ on the spacing between bead and glass surface, h-a, indicates that the increase of spacing drastically increases $\boldsymbol{F_D}$ (data is not shown). Figure 6 shows torques calculated in the same manner. Results for torque do not show difference between two models. Therefore, $\boldsymbol{F_D}$ was determined by the latter model (Fig. 3b) in the following discussion. Figure 7 shows ATP concentration dependency of the percentage of remaining number of beads to the initial number of beads. Clearly, solutions with high ATP concentrations break bindings at low $\boldsymbol{F_D}$ (low flow rate) because most kinesins are expected to be in unbound state to MT. We adopted a flow rate for $\boldsymbol{F_D}$ when 50% of microbeads were removed. For example, $\boldsymbol{F_{D(50\%)}}$ = 4.1 pN under 1 mM ATP concentration was used to derive $\boldsymbol{F_{Adh}}$ by equation (5). Other parameters used in the calculation were l_c=133 nm and w=30 nm. Calculated $\boldsymbol{F_{Adh}}$ is shown in Fig. 8. Average net adhesion forces are 362.9 pN, 348.3 pN, 335.3 pN, and 31.3 pN in no ATP, 10 μM ATP, 100 μM ATP, and 1 mM ATP concentrations, respectively. We could not find the force dependency on ATP concentrations below 100 μM, however, 1 mM ATP solution showed bead removal at low flow rate. Assuming all kinesins are active under 1 mM ATP and stall force of 5.8 pN per kinesin [8], 5.4 kinesin molecules are cooperatively working to carry a microbead. Such a nanotransport supported by multiple kinesins has been studied in vivo [9] and in vitro [10]. Reported number of kinesins involved in the transport is 5~10, so that our result falls in the same range.

CONCLUSION

Even though the proposed method has much lower spatial and temporal resolution than that in the optical tweezers method, the measured values are in the comparable range. Since we have not controlled the number of kinesins on a bead, it is still hard to discuss the force generated by single kinesin molecule. However, our method has possibility to derive the force, once we determine the number of kinesin molecules bridging the bead and MT. It does not provide us high resolution, because there are some uncertainties in the calculation. For example, the ratio of cooperatively working kinesins and inactive kinesins is unknown, and all kinesins are not in the same state of their walking steps. However, the averaged binding force was statistically measured depending on ATP concentrations. The relationship between the flow rate and the binding force is derived, so that the highest flow rate can be determined to avoid releasing beads from the

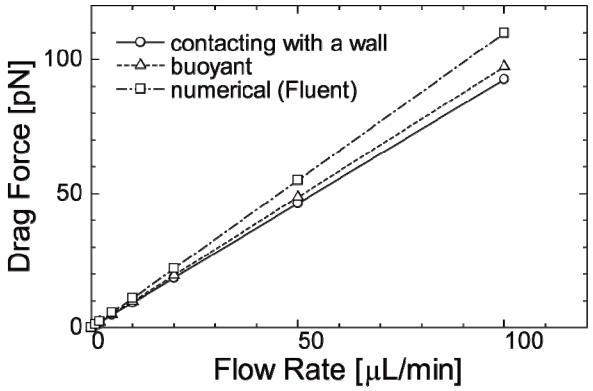

Figure 5: Drag force acting on a microbead (2a=1 μm, h=545 nm) derived by three calculation methods. Open circles (contacting with a wall) and triangles (buoyant) represent F_{D1} and F_{D2}, respectively.

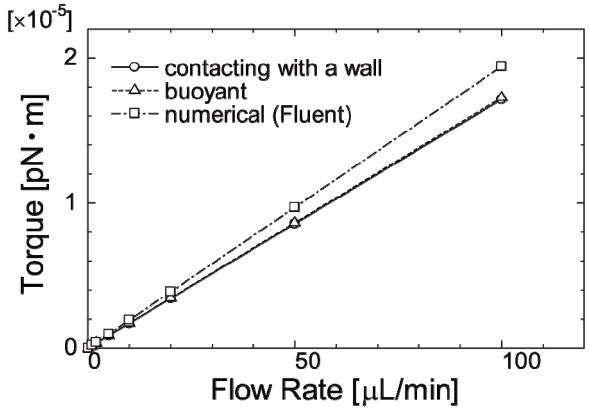

Figure 6: Torque acting on a microbead (2a=1 μm, h=545 nm) derived by three calculation methods. Open circles (contacting with a wall) and triangles (buoyant) represent Γ_1 and Γ_{D2}, respectively.

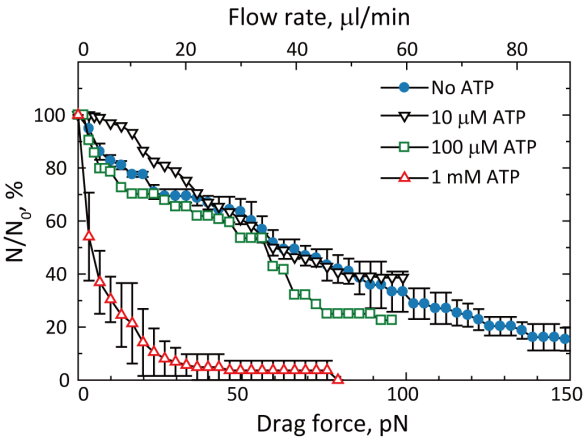

Figure 7: Percentage of remaining number of beads depending on flow rate for four ATP concentrations. Corresponding drag force calculated by microfluidic model (Fig. 3b) is also indicated.

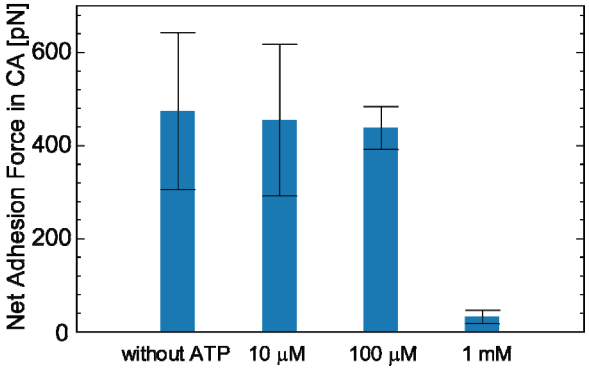

Figure 8: Net adhesion force depending on ATP concentrations calculated by experimental results and mechanical modeling.

glass surface. The result can be utilized to design a nanotransport system supported by the integration of kinesin-MT interactions and microfluidic systems.

ACKNOWLEDGEMENTS

This study was partially supported by Precursory Research for Embryonic Science and Technology (PRESTO) from Japan Science and Technology Agency (JST).

REFERENCES

[1] S. M. Block et al., Nature, vol. 348, pp. 348-52, 1990.
[2] M. O'Neill, Chem. Eng. Sci, vol. 23, pp. 1293-1298, 1968.
[3] A. Goldman et al., Chem. Eng. Sci, vol. 22, pp. 653-660, 1967.
[4] S. Lorthois et al., J. Colloid Interface Sci., vol. 241, pp. 52-62, 2001.
[5] R. Yokokawa et al., Nano. Lett., vol. 4, pp. 2265-2270, 2004.,
R. C. Williams et al., Methods Enzymol., vol. 85 Pt B, pp. 376-85, 1982.
[6] R. Yokokawa et al., Nano. Lett., vol. 4, pp. 2265-2270, 2004.
[7] J. Beeg et al., Biophys. J., vol. 94, pp. 532-541, 2008.
[8] J. Howard, Mechanics of Motor Proteins and the Cytoskeleton, Sinauer Associates Inc., 2001.
[9] A. Ashkin et al., Nature vol. 348, pp. 346-348, 1990.
[10] C. Bottier et al., Lab Chip, vol 9, pp. 1694-1700, 2009.

CONTACT

*R. Yokokawa, tel: +81-75-7533559; ryuji@me.kyoto-u.ac.jp